JOURNAL OF MOLECULAR SPECTROSCOPY **134,** 421–432 (1989)

Diode-Laser Spectroscopy of Alkali Halides: The Lithium Bromide Molecule

C. R. BRAZIER, N. H. OLIPHANT, AND P. F. BERNATH[1]

Department of Chemistry, University of Arizona, Tucson, Arizona 85721

The vibration–rotation spectrum of the lithium bromide molecule has been recorded using a tunable diode laser. A total of 1004 lines for all four isotopic combinations $^{6}Li^{79}Br$, $^{6}Li^{81}Br$, $^{7}Li^{79}Br$, and $^{7}Li^{81}Br$ in eight $\Delta v = 2$ overtone bands were observed. The lines were fitted to Dunham and mass-reduced Dunham parameters.

INTRODUCTION

The alkali halides were studied extensively during the 1950s and 1960s by microwave spectroscopy (*1–4*) partly because of their very large dipole moments (5–12 D) and reasonable vapor pressures at moderately elevated temperatures. Since that time, there was no rotationally resolved work on any of the alkali halides until very recently. The advent of high resolution Fourier transform spectrometers and diode lasers has made possible the observation of infrared vibration–rotation spectra of the alkali halides. Much of the work has been performed by Maki and co-workers (*5–8*) who studied all of the lithium halides except LiBr as well as potassium fluoride. Very recently, Jones and Lindenmayer (*9*) have made further observations on LiCl while Horiai *et al.* (*10*) have studied NaCl. As part of the present study, the spectrum of NaF was recorded by Douay *et al.* (*11*).

The early microwave work on lithium bromide (*1–3*) gave very precise values for the rotational constants, which were extremely useful in assigning the present measurements. This work also provided information on the hyperfine interactions and more extensive hyperfine measurements were made by Ramsey and co-workers (*12*). While the vibrational frequency was obtained only indirectly from the microwave data, the value obtained of $\omega_e = 563.5 \pm 2.2\ \mathrm{cm^{-1}}$ for $^{7}Li^{79}Br$ (*2*) compares favorably with the value of $562.283\ \mathrm{cm^{-1}}$ determined in our work. Predictions of the vibrational frequency were also available from the low resolution infrared studies of Klemperer and co-workers (*13, 14*). Their value of $\omega_e = 563.2 \pm 0.2\ \mathrm{cm^{-1}}$ was also very close, although outside of their rather small error limits. These estimates of the vibrational frequency were very useful in determining where to search at high resolution.

The visible and UV spectra of the alkali halides consist of continua and fluctuation bands (*15*). Only for sodium iodide have discrete rotationally resolved spectra been observed (*16, 17*). The continuum absorption for LiBr was described by Davidovits and Brodhead (*18*), and the fluctuation bands by Berry and Klemperer (*19*).

[1] Alfred P. Sloan Fellow; Camille and Henry Dreyfus Teacher Scholar.

0022-2852/89 $3.00

The first ionization potential of LiBr has been determined by Potts and Lee (*20*) and Berkowitz *et al.* (*21*) to be 9.3 eV by photoelectron spectroscopy. A value of 4.4 eV for the bond dissociation energy has been found from thermodynamic (*22*) and flame photometric (*23*) measurements.

Theoretical calculations on LiBr have so far been made only at the SCF level (*24, 25*). The results of Matcha (*24*), as part of a systematic study of the alkali halides, are fairly good for the main spectroscopic parameters, but the higher order constants (which were previously unmeasured) do not compare well with the current experimental results. Lithium bromide, along with the other alkali halides, has been the subject of numerous (*26–32*) empirical calculations using various formulations of the Rittner potential (*33*). Other types of potentials such as the ionic Kratzer-type potential have also been used (*34*).

EXPERIMENTAL DETAILS

Lithium bromide vapor was produced in a stainless steel heat pipe oven. This consisted of a 1-m-long, 50-mm-diameter tube with a gas inlet at one end and pump outlet at the other. BaF_2 windows on each end of the tube allowed transmission of the infrared radiation. The LiBr vapor was prevented from reaching the windows by pressurizing the tube with 5 Torr of argon. About 100 g of LiBr was placed on stainless steel gauze in the center part of the tube and heated by a cylindrical furnace to about 1100 K resulting in about 5 Torr of LiBr vapor. The ends of the tube were water cooled and this, together with the argon, helped contain the LiBr vapor to the center 0.5-m region of the cell. The oven acted as a heat pipe and could be repeatedly heated and cooled over a period of weeks without adding fresh LiBr.

The output from a lead salt diode laser (Laser Analytics) was multipassed eight times through the oven, using external White cell-type optics. The beam was then passed through a 1/3-m monochromator to select a single longitudinal mode of the laser and was focused onto a liquid nitrogen cooled Hg-Cd-Te detector. Absolute calibration of the spectrum was obtained by placing a 20-cm cell containing ammonia in the beam path. The $^{14}NH_3$ lines were observed with a cell containing 200 mTorr of NH_3; $^{15}NH_3$ lines were observed in natural abundance at a pressure of 5 Torr. The lines were compared with the published spectrum of NH_3 (*35*). A part of the beam was picked off with a beam splitter and passed through an air-spaced germanium etalon, with a 0.03 cm^{-1} free spectral range, to provide relative frequency calibration.

Several $\Delta v = 2$ bands of LiBr were measured between 1030 and 1120 cm^{-1} by frequency modulating the diode at 4 kHz and recording the signal with a lock-in amplifier at twice the modulation frequency. The molecular signal and the etalon markers, recorded using 1-f modulation, were output simultaneously on a two-pen chart recorder.

RESULTS AND DISCUSSION

The lines of the 2–0 band of LiBr were predicted using the microwave (*1, 2*) and low resolution infrared measurements (*14*) and a search for the strong *P*-branch lines was made near 1070 cm^{-1}. A very dense spectrum with an *R*-branch bandhead similar to that in Fig. 1 was observed. The bandhead was assigned to the 6–4 band of the

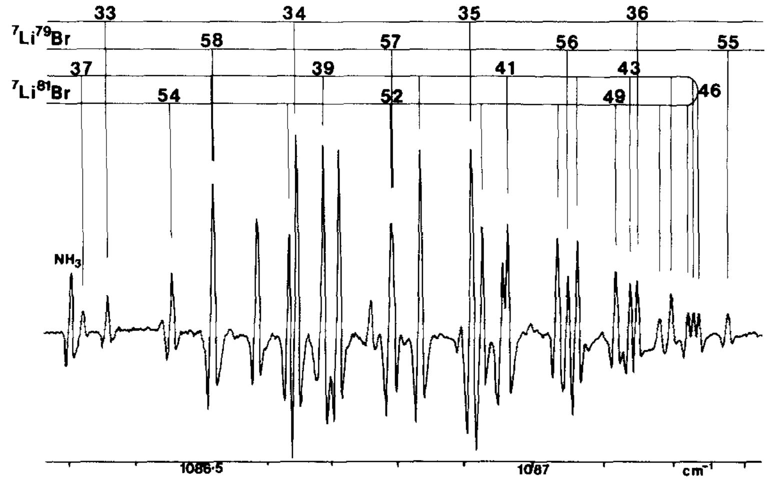

FIG. 1. A section of the lithium bromide spectrum near the 5–3 bandhead. Lines for the $^7Li^{81}Br$ isotopomer at the bandhead and also for the $^7Li^{79}Br$ isotopomer are indicated. Unmarked lines are from the 2–0, 3–1, and 4–2 bands. A single ammonia calibration line is also shown.

$^7Li^{79}Br$ isotope, but clearly the lines were as strong as for the 2–0, 3–1, etc. bands. As the population of the higher vibrational levels falls by about a factor of 2 for each level, the transition strength must be increasing with vibration to compensate for this. A discussion of the relative intensities of the overtone bands will be presented later.

Once the first LiBr lines had been obtained and the intensity pattern understood, recording and assignment of further lines was relatively easy. The J assignment for the bandheads could be made using the microwave constants (*1, 2*) and the remaining lines could then be assigned by fitting the lines near the bandheads and predicting the rest of the spectrum. The upper frequency limit of the diode was 1120 cm^{-1} which covered the region near the 2–0 bandhead. Measurements were made down to 1030 cm^{-1}. This covered the $\Delta v = 2$ bands up to 9–7. Further bands could have been recorded, but by this point it was found that the line positions could be predicted almost as precisely as they could be measured.

A section of the LiBr spectrum near the 5–3 bandhead for the $^7Li^{81}Br$ isotope is shown in Fig. 1. The two isotopes are present in almost equal proportions which adds to the complexity of the spectrum. The strong transitions absorb about 2% of the infrared radiation which results in a signal-to-noise ratio of around 50. This should yield very precise line positions given the 0.005 cm^{-1} linewidth, but the use of a chart recorder to record the lines and the lack of sufficient calibration lines limit the precision of the measurements to about 0.0025 cm^{-1}.

Nine hundred and fifty lines belonging to the two main isotopic species $^7Li^{79}Br$ (47%) and $^7Li^{81}Br$ (45.6%) were recorded and fitted to the Dunham energy level expression (*36*). The line positions and errors are given in Table I. Each isotope was initially fitted separately and the Dunham Y coefficients obtained are given in Table II. The microwave transitions of Honig *et al.* (*1*) and Rusk and Gordy (*2*) were included in the fit. The hyperfine free line positions were calculated from the observed transitions using the published hyperfine constants (*1–3, 12*). It was found that the

TABLE I

Observed Lines in the Vibration–Rotation Spectrum of LiBr (in cm^{-1})

$^{7}Li^{81}Br$

P(J)	2-0 ν	2-0 Δν[a]	3-1 ν	3-1 Δν	4-2 ν	4-2 Δν	5-3 ν	5-3 Δν	6-4 ν	6-4 Δν	7-5 ν	7-5 Δν
1												
2			1086.760	0	1073.275	0					1033.790	-2
3	1099.260	-2	1085.621	-3	1072.150	-1			1045.693	2		
4			1084.466	-0	1071.004	-1	1057.705	-1	1044.567	-2		
5	1096.903	1	1083.285	-2	1069.839	2	1056.549	-1	1043.425	1		
6					1068.652	4	1055.375	2				
7	1094.454	1			1067.435	-3	1054.175	0	1041.072	-1		
8	1093.195	-1	1079.621	2	1066.209	3	1052.954	-1	1039.868	3		
9	1091.916	-2	1078.355	2	1064.952	-0	1051.712	-2	1038.637	0		
10	1090.626	9			1063.675	-2	1050.449	-3				
11	1089.292	-3	1075.757	1	1062.383	2	1049.169	0				
12			1074.425	-0	1061.068	4	1047.870	5	1034.825	-0		
13	1086.583	-3	1073.077	3			1046.539	-0	1033.513	-0		
14	1085.200	1	1071.700	-0	1058.365	-1	1045.193	-0	1032.181	0		
15	1083.793	2	1070.304	-2	1056.984	-1	1043.831	5				
16			1068.894	4								
17			1067.451	-3	1054.161	0	1041.028	-2				
18	1079.438	0	1065.995	-1	1052.717	-0	1039.603	2				
19			1064.517	0	1051.251	-2	1038.147	-4				
20	1076.425	-5	1063.015	-2								
21			1061.501	4	1048.268	6	1035.186	-3				
22	1073.335	-2			1046.733	-3	1033.673	-5				
23	1071.757	-3	1058.393	0	1045.187	-2	1032.145	-1				
24	1070.159	-2	1056.807	-3	1043.624	3						
25	1068.543	1	1055.207	1								
26	1066.900	-1	1053.579	-3	1040.422	-3						
27	1065.243	2	1051.935	-2	1038.799	2						
28	1063.556	-3	1050.270	-2								
29	1061.856	-1			1035.475	-4						
30	1060.135	1	1046.879	-2	1033.792	3						
31	1058.393	2	1045.151	-4	1032.077	-3						
32	1056.627	-1	1043.407	-1								
33	1054.846	2										
34	1053.039	-1	1039.856	0								
35	1051.214	-2										
36	1049.370	-2										
37	1047.509	1	1034.378	1								
38	1045.622	-2										
39	1043.723	3										
40												
41	1039.856	4										
42												
43												
44	1033.906	2										

R(J)	2-0 ν	2-0 Δν	3-1 ν	3-1 Δν	4-2 ν	4-2 Δν	5-3 ν	5-3 Δν	6-4 ν	6-4 Δν	7-5 ν	7-5 Δν	8-6 ν	8-6 Δν	9-7 ν	9-7 Δν
0			1090.039	4	1076.513	-4	1063.158	-5								
1							1064.189	-0	1050.983	-3						
2			1092.110	2	1078.574	5	1065.198	4	1051.979	-1	1038.926	0				
3			1093.112	1	1079.564	2	1066.181	4	1052.954	1	1039.894	5				
4			1094.092	-1			1067.137	-1	1053.904	-0	1040.830	-0				
5							1068.077	0	1054.835	1						
6			1095.986	-2			1068.996	2			1042.644	-4				
7			1096.903	1	1083.311	-3	1069.891	1	1056.627	-0	1043.527	2				
8			1097.794	-0	1084.197	1	1070.762	-1	1057.490	-2						
9					1085.057	0	1071.614	-0	1058.334	0	1045.212	-2				
10	1113.290	-2	1099.510	-0	1085.897	3	1072.447	4			1046.025	-0	1033.056	1		
11	1114.123	-2	1100.332	-2	1086.712	2	1073.251	1			1046.814	-1	1033.834	-2		
12	1114.941	5	1101.139	3	1087.507	4	1074.032	-3	1060.729	-0	1047.586	2	1034.599	3		
13							1074.788	-9	1061.489	6			1035.333	-2		
14					1089.025	3	1075.538	0	1062.217	1	1049.053	-1				
15			1103.400	-5	1089.751	3	1076.252	-4	1062.924	-2						
16			1104.118	2	1090.458	7			1063.610	-4	1050.434	-3				
17					1091.142	9			1064.277	-3						
18							1078.274	-1	1064.922	-1	1051.728	-4	1038.703	3		
19					1092.422	-3	1078.904	1	1065.543	-1	1052.350	3	1039.309	1		
20					1093.037	-0	1079.510	1	1066.146	3	1052.937	-2	1039.894	1		
21					1093.630	3			1066.715	-5	1053.505	-4	1040.455	-2		
22					1094.193	-1			1067.274	0	1054.057	0	1040.996	-3		
23									1067.804	-2	1054.585	3				
24									1068.318	3	1055.087	1				
25					1095.752	-5			1068.805	4						
26	1123.860	-2			1096.232	-0			1069.267	1			1042.943	-1		
27	1124.324	-2			1096.686	1	1083.114	-0	1069.711	4	1056.460	-1	1043.375	-0		
28	1124.768	3			1097.116	2	1083.538	-0	1070.125	-1	1056.872	-3	1043.789	5		
29					1097.518	-2	1083.940	1	1070.521	-1	1057.265	-2				
30					1097.906	3	1084.320	2	1070.894	-2	1057.634	-2				
31							1084.673	-0	1071.248	1	1057.983	1	1044.875	-2		
32							1085.003	-3	1071.575	0	1058.306	0	1045.193	-3		
33							1085.315	0	1071.880	0			1045.490	-4		
34					1099.202	-2	1085.600	-1	1072.159	-3			1045.769	1		
35			1113.244	-0	1099.468	-4	1085.867	2	1072.426	4			1046.025	4	1033.056	-2
36			1113.490	-2	1099.714	-1	1086.106	1	1072.660	1					1033.286	2
37			1113.715	-1	1099.933	-3	1086.322	-0	1072.873	0			1046.457	-1	1033.489	0
38			1113.917	0	1100.131	-2	1086.517	1	1073.068	4			1046.640	-3	1033.673	2
39			1114.092	-1	1100.308	1	1086.685	-2	1073.230	-2			1046.803	-2	1033.834	4
40			1114.246	-1	1100.458	0	1086.835	-0	1073.377	0			1046.944	-1	1033.969	2
41			1114.375	-1	1100.584	-1	1086.958	-2	1073.500	1	1060.202	2	1047.063	1	1034.082	-0
42			1114.483	1	1100.686	-2	1087.063	2	1073.599	1	1060.298	1	1047.158	1	1034.172	-3
43			1114.564	-1	1100.767	-1	1087.141	2	1073.673	-1	1060.372	1	1047.231	2		
44			1114.623	-0	1100.824	-1	1087.192	-2	1073.726	-1	1060.422	-0	1047.280	2	1034.293	0
45			1114.657	-1	1100.860	2	1087.222	-3	1073.753	-3	1060.452	2	1047.306	1	1034.320	3
46			1114.672	3	1100.869	1	1087.231	-2	1073.759	-4	1060.455	-0	1047.309	1	1034.320	0
47			1114.657	0	1100.854	0	1087.216	-2	1073.744	-2	1060.437	-1	1047.292	2	1034.302	2
48			1114.623	3	1100.815	-1	1087.180	1	1073.708	1	1060.397	-0	1047.250	2	1034.257	-0
49			1114.564	4	1100.752	-3	1087.120	3	1073.644	0	1060.334	1	1047.185	2	1034.191	-1

[a] in units of 10^{-3} cm^{-1}.

TABLE I—*Continued*

R(J)	2-0 ν	2-0 Δν	3-1 ν	3-1 Δν	4-2 ν	4-2 Δν	5-3 ν	5-3 Δν	6-4 ν	6-4 Δν	7-5 ν	7-5 Δν	8-6 ν	8-6 Δν	9-7 ν	9-7 Δν
50			1114.480	4	1100.668	-2	1087.033	1	1073.560	2	1060.248	1	1047.096	-0	1034.104	-0
51			1114.367	-1	1100.563	1	1086.925	2	1073.449	0	1060.137	-0	1046.986	-0	1034.000	6
52			1114.236	-1	1100.428	-2	1086.793	2	1073.317	1			1046.849	-4	1033.863	2
53			1114.082	1	1100.272	-2	1086.634	-1	1073.161	1			1046.696	-2	1033.704	-2
54			1113.903	2	1100.092	-3	1086.454	-1	1072.984	3			1046.516	-3	1033.527	-0
55			1113.698	0	1099.891	-1	1086.253	0	1072.780	1					1033.324	-3
56			1113.470	-0	1099.663	-2	1086.025	-1	1072.552	-1						
57			1113.219	0	1099.415	1	1085.777	0	1072.303	-1			1045.844	-2		
58					1099.138	-2	1085.501	-2	1072.033	1			1045.575	-1		
59							1085.207	1	1071.736	-0			1045.276	-7		
60							1084.883	-3	1071.417	-0	1058.112	0	1044.964	-3		
61							1084.541	-1	1071.074	-1	1057.768	-3	1044.625	-3		
62					1097.804	-0	1084.174	0	1070.709	0	1057.406	-1				
63					1097.407	-4	1083.784	1	1070.318	-2	1057.016	-4	1043.886	4		
64					1096.996	3	1083.365	-3	1069.912	5	1056.609	-1	1043.474	0		
65	1124.306	2			1096.551	-1	1082.931	2	1069.473	2			1043.044	1		
66	1123.834	1			1096.087	-0			1069.013	1			1042.596	7		
67									1068.531	2	1055.241	1				
68									1068.021	-2						
69					1094.550	1			1067.488	-5	1054.209	-2				
70					1093.985	-4			1066.939	-1	1053.659	-2	1040.540	-4		
71					1093.403	-1	1079.804	3	1066.361	-2	1053.089	0	1039.977	2		
72					1092.798	2	1079.198	1	1065.758	-5						
73					1092.164	-0	1078.574	5	1065.142	3						
74									1064.493	0						
75					1090.833	5			1063.821	-1						
76			1103.874	1	1090.128	4			1063.123	-5						
77			1103.138	-2	1089.397	0			1062.413	2						
78					1088.647	2			1061.669	-1						
79									1060.908	2						
80			1100.797	0	1087.075	5			1060.119	1						
81			1099.966	-1												
82																
83																
84			1097.335	0												
85			1096.411	2												
86																
87																
88																
89			1092.463	-1												

$^{7}Li^{79}Br$

P(J)	2-0 ν	2-0 Δν	3-1 ν	3-1 Δν	4-2 ν	4-2 Δν	5-3 ν	5-3 Δν	6-4 ν	6-4 Δν	7-5 ν	7-5 Δν
1					1075.415	2						
2					1074.314	5	1060.959	-2				
3					1073.182	-0			1046.670	-1	1033.653	-3
4	1099.175	-1	1085.522	-0	1072.033	-1			1045.546	0		
5			1084.341	1	1070.862	-2	1057.551	-0				
6	1096.765	-1	1083.138	1	1069.678	5	1056.369	-3	1043.232	0		
7					1068.460	0	1055.172	1				
8	1094.268	-1			1067.223	-2	1053.948	-0	1040.830	-3		
9	1092.987	-1	1079.396	0	1065.968	-1	1052.703	-2	1039.603	1		
10			1078.103	-2	1064.693	2	1051.438	-2	1038.349	-1		
11	1090.366	7			1063.388	-4	1050.152	-2				
12	1089.013	1	1075.460	0	1062.075	3	1048.845	-2	1035.775	-7		
13	1087.650	6	1074.104	-1	1060.729	-2	1047.521	2	1034.469	2		
14	1086.253	-1	1072.732	3			1046.171	1	1033.133	1		
15	1084.841	-2	1071.333	2	1057.983	-1	1044.798	-2				
16	1083.410	0	1069.912	-1	1056.579	-1	1043.407	-2				
17			1068.479	6								
18			1067.011	-1	1053.705	-2	1040.562	-3				
19	1078.985	2	1065.530	1	1052.242	2	1039.109	-3				
20			1064.025	-1	1050.751	-0						
21	1075.927	1	1062.506	4	1049.240	-2						
22	1074.365	-1	1060.959	2	1047.715	3	1034.629	0				
23	1072.786	2			1046.163	2	1033.091	-2				
24	1071.183	1	1057.802	-3	1044.588	-2						
25	1069.561	2			1042.999	0						
26	1067.913	-2	1054.571	2	1041.387	0						
27	1066.252	2	1052.918	-3	1039.756	2						
28	1064.564	-1	1051.251	-1	1038.095	-7						
29	1062.855	-4	1049.562	-0								
30	1061.137	5	1047.857	5	1034.735	-0						
31			1046.122	-0	1033.022	-0						
32	1057.614	-3										
33			1042.596	-5								
34	1054.022	1	1040.807	-4								
35	1052.194	1	1039.000	0								
36	1050.343	-1										
37			1035.316	-3								
38	1046.585	-2	1033.445	-3								
39	1044.676	-2										
40	1042.745	-5										
41	1040.807	6										
42	1038.835	2										
43												
44	1034.837	-1										

R(J)	2-0 ν	2-0 Δν	3-1 ν	3-1 Δν	4-2 ν	4-2 Δν	5-3 ν	5-3 Δν	6-4 ν	6-4 Δν	7-5 ν	7-5 Δν	8-6 ν	8-6 Δν	9-7 ν	9-7 Δν
0							1064.175	-2								
1			1092.149	-3	1078.601	5	1065.209	4	1051.979	3	1038.909	3				
2			1093.180	1	1079.619	6	1066.209	-3	1052.971	-1	1039.896	4				
3			1094.186	2			1067.196	-0	1053.948	1	1040.854	-3				
4							1068.159	-0	1054.903	3						
5			1096.128	-0			1069.104	4			1042.718	-4				
6			1097.068	2	1083.460	-1	1070.019	-0	1056.741	1	1043.624	2				
7					1084.370	3	1070.917	1	1057.625	-3						
8					1085.252	1	1071.790	-1			1045.354	-3				

TABLE I—*Continued*

R(J)	2-0 ν	Δν	3-1 ν	Δν	4-2 ν	Δν	5-3 ν	Δν	6-4 ν	Δν	7-5 ν	Δν	8-6 ν	Δν	9-7 ν	Δν
9	1113.547	-0	1099.747	0	1086.115	2	1072.642	-2					1033.205	1		
10	1114.404	-1	1100.596	1	1086.958	6	1073.476	2	1060.160	1	1047.005	0				
11					1087.777	8	1074.281	-1	1060.959	0	1047.799	3	1034.792	0		
12					1088.569	6	1075.068	-0	1061.736	-0			1035.550	-3		
13			1103.002	-2	1089.337	2	1075.832	-0	1062.495	3	1049.312	-1				
14			1103.761	-0	1090.089	4	1076.568	-6	1063.219	-6	1050.039	1				
15					1090.818	6			1063.936	-1	1050.742	0				
16									1064.626	0	1051.422	-1	1038.379	-1		
17					1092.197	-0	1078.670	7	1065.297	5	1052.084	1	1039.033	1		
18					1092.858	2	1079.312	-3	1065.935	-2	1052.717	-3	1039.665	2		
19					1093.492	-0	1079.948	4	1066.558	-1	1053.335	-0	1040.267	-4		
20					1094.106	1			1067.154	-4	1053.926	-2	1040.854	-3		
21									1067.733	-2	1054.500	1				
22									1068.287	-3	1055.048	1				
23					1095.804	-4			1068.826	4						
24	1123.992	1			1096.328	-1			1069.334	2			1042.982	1		
25	1124.501	-0			1096.828	0	1083.240	-1	1069.821	2	1056.557	-1	1043.459	2		
26					1097.302	-2	1083.710	-1	1070.281	-2	1057.016	-1	1043.916	5		
27					1097.755	-1	1084.159	0	1070.725	-0	1057.453	-1				
28							1084.583	0	1071.145	1	1057.867	-1	1044.747	-4		
29							1084.982	-2	1071.540	-0	1058.259	0	1045.134	-3	1032.175	1
30							1085.363	1	1071.913	-1			1045.502	0		
31					1099.333	-2	1085.717	-1	1072.258	-7			1045.844	0		
32			1113.458	-2	1099.672	0	1086.046	-4	1072.591	-2			1046.163	-0	1033.185	-1
33			1113.778	0	1099.984	-1	1086.358	-1	1072.900	2			1046.457	-3	1033.479	-0
34			1114.072	-0	1100.272	-3	1086.643	-3	1073.182	2			1046.733	-2	1033.755	5
35			1114.342	-1	1100.544	2	1086.910	1	1073.440	0	1060.135	2	1046.986	-1	1034.000	1
36			1114.591	1	1100.782	-4	1087.150	1	1073.673	-3	1060.368	2	1047.217	1	1034.224	-1
37			1114.813	-0	1101.007	1	1087.366	1	1073.882	-7	1060.576	-0	1047.425	2	1034.432	3
38			1115.015	2	1101.205	2	1087.564	5	1074.077	-3	1060.763	-0	1047.609	1	1034.611	1
39					1101.379	3	1087.738	9	1074.245	-2	1060.929	1	1047.772	3	1034.768	-1
40							1087.882	6	1074.392	0	1061.072	2	1047.910	2	1034.904	-2
41							1087.986	-14	1074.512	-1	1061.194	5	1048.027	2	1035.016	-4
42							1088.083	-18	1074.605	-6	1061.289	5	1048.121	2	1035.108	-3
43							1088.167	-11	1074.677	-9	1061.364	7	1048.193	3	1035.179	-1
44							1088.221	-10	1074.728	-10	1061.413	5	1048.243	5	1035.225	-2
45							1088.254	-8	1074.755	-12	1061.440	5	1048.268	4	1035.250	-1
46							1088.266	-3	1074.761	-11	1061.442	3	1048.268	2	1035.250	-3
47							1088.242	-10	1074.743	-12	1061.424	4	1048.252	6	1035.229	-2
48							1088.203	-10	1074.704	-10	1061.383	5	1048.208	5	1035.186	-2
49							1088.137	-12	1074.644	-6	1061.318	5	1048.140	2	1035.117	-4
50							1088.047	-15	1074.557	-5	1061.230	5	1048.052	3	1035.028	-4
51							1087.942	-10	1074.449	-2	1061.118	4	1047.940	2	1034.918	-3
52							1087.828	10	1074.314	-3	1060.980	0	1047.806	2	1034.785	-1
53					1101.331	4	1087.666	5	1074.158	-2	1060.820	-3	1047.647	1	1034.629	-0
54			1114.983	3	1101.148	2	1087.483	3	1073.975	-4	1060.640	-2	1047.468	2	1034.452	3
55			1114.775	0	1100.938	-3	1087.276	1	1073.774	-1	1060.437	-2	1047.265	2		
56			1114.547	2	1100.710	-3	1087.051	4	1073.548	0	1060.213	1	1047.036	-1		
57			1114.291	-1	1100.458	-2	1086.793	-3	1073.296	-1			1046.785	-3	1033.774	0
58			1114.015	0	1100.182	-2	1086.517	-3	1073.026	3			1046.516	-0	1033.501	-2
59			1113.715	2	1099.882	-1	1086.223	2	1072.729	4					1033.205	-4
60			1113.385	-3	1099.558	-1	1085.897	-2	1072.408	4			1045.902	-1		
61					1099.210	-1	1085.552	-0	1072.060	1			1045.561	-1		
62							1085.183	0	1071.691	-0	1058.365	1				
63							1084.790	1	1071.301	1	1057.971	-4	1044.809	-2		
64							1084.370	-2	1070.883	-2	1057.561	-1				
65					1097.581	0	1083.931	0	1070.446	-1	1057.126	-0	1043.972	4		
66					1097.116	3	1083.460	-6	1069.985	0	1056.665	-2	1043.512	0		
67	1124.417	1			1096.621	-1	1082.979	1	1069.502	3	1056.183	-2	1043.032	-0		
68	1123.897	2			1096.104	-2			1068.996	6						
69									1068.460	2						
70									1067.902	-0	1054.600	2				
71					1094.417	1			1067.321	-2	1054.022	-1				
72					1093.804	-1			1066.715	-5	1053.424	0				
73					1093.170	-0	1079.549	0	1066.095	2	1052.801	-1				
74					1092.508	-3			1065.443	-0	1052.158	2				
75							1078.214	-2	1064.770	1	1051.486	-1				
76									1064.070	-2						
77			1104.164	4	1090.398	8			1063.347	-5						
78					1089.637	2			1062.612	4						
79					1088.854	-2			1061.841	1						
80									1061.051	2						
81			1100.971	-2					1060.238	4						
82			1100.114	-2												
83			1099.231	-4												
84																
85			1097.395	-4												

$^{6}Li^{81}Br$

P(J)	2-0 ν	Δν	3-1 ν	Δν	4-2 ν	Δν	5-3 ν	Δν	6-4 ν	Δν
25							1097.232	-2		
26										
27							1093.462	1	1078.781	2
28										
29							1089.589	-1	1074.948	-1
30										
31							1085.621	0		
32			1113.340	-2						
33					1096.306	0				
34					1094.213	-2				
35										
36					1089.961	1			1060.784	-0
37										
38							1070.968	-2		
39					1083.398	-0				
40			1095.948	-3						
41			1093.670	1			1064.335	-0		
42										
43										
44					1071.988	0				

TABLE I—*Continued*

$^{6}Li^{81}Br$

P(J)	2-0 ν	2-0 Δν	3-1 ν	3-1 Δν	4-2 ν	4-2 Δν	5-3 ν	5-3 Δν	6-4 ν	6-4 Δν
45			1084.304	2	1069.640	5				
46					1067.258	-2				
47	1094.291	-0			1064.861	-0				
48					1062.443	3				
49										
50			1072.066	-2	1057.528	0				
51										
52										
53										
54	1076.492	-3								

$^{6}Li^{79}Br$

P(J)	2-0 ν	2-0 Δν	3-1 ν	3-1 Δν	4-2 ν	4-2 Δν	5-3 ν	5-3 Δν	6-4 ν	6-4 Δν	7-5 ν	7-5 Δν
20									1092.269	1		
21												
22									1088.775	-0		
23											1072.396	-3
24												
25												
26							1096.218	1				
27							1094.318	3			1065.097	2
28							1092.383	-5				
29									1075.771	1		
30							1088.455	-4				
31					1101.280	3			1071.835	-0		
32			1114.222	-3								
33					1097.161	1						
34												
35					1092.948	3						
36							1076.090	-2				
37					1088.635	2						
38					1086.441	-0	1071.778	-0				
39					1084.228	2	1069.588	3				
40			1096.798	-1			1067.367	-2				
41					1079.723	0	1065.131	2				
42												
43			1089.868	2	1075.125	-0						
44			1087.507	-0								
45			1085.126	1	1070.436	2						
46					1068.053	-0						
47												
48	1092.649	-1										
49					1060.773	-0						
50												
51			1070.346	3								

TABLE II

Dunham Parameters for $^{7}Li^{79}Br$ and $^{7}Li^{81}Br$ (in cm^{-1})

Constant	$^{7}Li^{79}Br$	$^{7}Li^{81}Br$
$Y_{10} = \omega_e$	562.28564 (78)	561.71538 (70)
$Y_{20} = -\omega_e x_e$	-3.51011 (27)	-3.50195 (25)
$Y_{30} = \omega_e y_e$	0.014363 (40)	0.014170 (37)
$10^5\ Y_{40} = \omega_e z_e$	-4.81 (21)	-4.05 (20)
$Y_{01} = B_e$	0.55539720 (36)	0.55427796 (42)
$Y_{11} = -\alpha_e$	-0.00564616 (57)	-0.00562876 (45)
$10^5\ Y_{21} = \gamma_e$	2.4952 (77)	2.4776 (66)
$10^8\ Y_{31}$	-4.77 (43)	-4.52 (39)
$10^6\ Y_{02} = -D_e$	-2.1678 (18)	-2.1634 (17)
$10^8\ Y_{12} = -\beta_e$	1.144 (19)	1.165 (16)
$10^{11}\ Y_{22}$	1.94 (75)	1.84 (64)
$10^{12}\ Y_{03} = H_e$	3.59 (53)	3.01 (45)

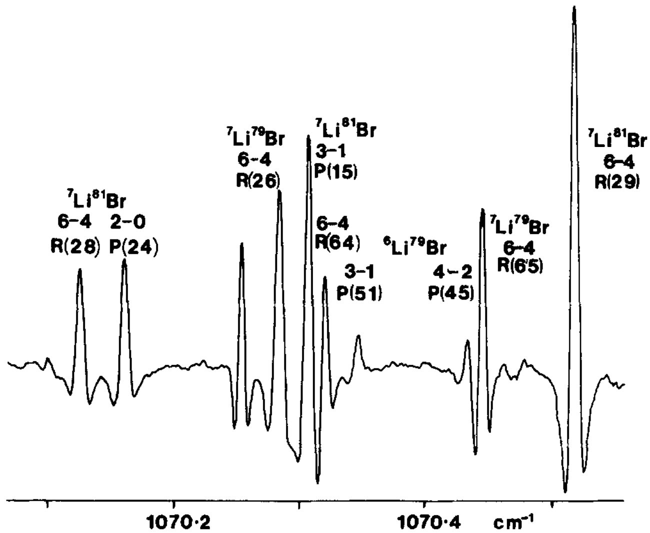

FIG. 2. A section of the lithium bromide spectrum, showing the essentially random appearance of the spectrum away from the bandheads. Also shown are two $^6Li^{79}Br$ lines in natural abundance (4%).

measurements of Honig *et al.* (*1*) did not fit with the other observations to within the published precision, so they were deweighted by a factor of 6. Small inconsistencies with the data of Honig *et al.* (*1*) were also reported by Hebert *et al.* (*3*) in their work on ^{6}LiBr.

TABLE III

Mass Reduced Dunham Constants for LiBr (in cm^{-1})

	U_{10}	1427.2689 (12)
	U_{20}	-22.6119 (11)
	U_{30}	0.23344 (42)
	U_{40}	-0.001822 (57)
	U_{01}	3.5784421 (93)
	Δ_{01}^{Li}	0.314 (29)
	U_{11}	-0.0923319 (31)
	U_{21}	0.0010327 (16)
10^6	U_{31}	-4.74 (27)
10^5	U_{02}	-9.0152 (30)
10^6	U_{12}	1.2083 (53)
10^9	U_{22}	6.21 (89)
10^{10}	U_{03}	9.77 (48)

TABLE IV

RKR Turning Points for the $X\,^1\Sigma^+$ State of $^7Li^{79}Br$

v	E_v(cm^{-1})	R_{min}(Å)	R_{max}(Å)
0	280.4123	2.07952	2.27301
1	835.7230	2.01957	2.35640
2	1384.1421	1.98124	2.41833
3	1925.7530	1.95174	2.47160
4	2460.6383	1.92737	2.51991
5	2988.8794	1.90645	2.56494
6	3510.5566	1.88803	2.60762
7	4025.7493	1.87154	2.64854
8	4534.5358	1.85660	2.68809
9	5036.9932	1.84291	2.72655

The data for the two isotopic species were then combined and fitted to the mass reduced Dunham expression including Watson's Born–Oppenheimer breakdown coefficients (*37*). All of the data could be fitted without the introduction of any of Watson's coefficients. The microwave lines of Hebert *et al.* (*3*) for ^{6}LiBr were then included and a prediction of the ^{6}LiBr vibration–rotation lines was made. ^{6}LiBr lines could not be picked out without this prediction because ^{6}Li is present at only 7.5%, in natural abundance, and the large shift in the vibrational frequency (ω_e = 562.28 cm^{-1} for $^7Li^{79}Br$, ω_e = 603.72 cm^{-1} for $^6Li^{79}Br$) meant that only the widely spaced *P*-branch lines could be seen in the region observed. Based on the prediction, a total of 59 ^{6}LiBr lines could be picked out from the existing spectra. These were all moderate to high *J*-, *P*-branch lines ranging from the 2–0 to the 7–5 bands for both isotopic species, $^6Li^{79}Br$ and $^6Li^{81}Br$. A typical section of the LiBr spectrum including two weak ^{6}LiBr lines is shown in Fig. 2.

The ^{6}LiBr vibration–rotation lines were then fitted with the rest of the observed transitions to mass-reduced Dunham coefficients. One of Watson's Δ's (*37*) was needed for the B_e (Y_{01}) rotational constant for lithium. This was due primarily to the high precision microwave data available for ^{6}LiBr. The results of this fit are given in Table III.

DISCUSSION

The vibration–rotation constants were used as input to an RKR program. The classical turning points are given in Table IV, and the lower part of the curve is shown in Fig. 3. The bands observed, up to $v = 9$, cover the first 15% of the potential well. The equilibrium bond length was calculated to be 2.17043 Å.

As was mentioned earlier, the intensities of the hot bands 3–1, 4–2, etc. are higher

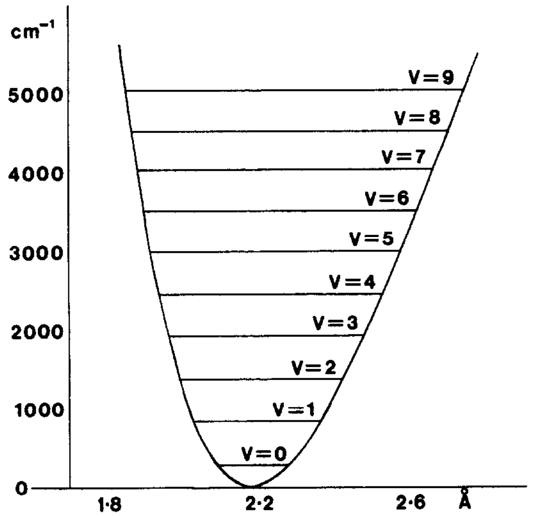

FIG. 3. The potential energy curve for $^{7}Li^{79}Br$. The equilibrium constants, from Table II, were used to calculate the RKR turning points.

than that of the 2–0 band. An estimate of the relative intensity of the bands was made from the diode-laser spectrum. This is difficult to do except where lines are very close together, because of the variation in diode-laser power. Initially, pairs of lines in a given band were measured, usually *R*-branch lines going into and coming out of a bandhead. From these data, the rotational temperature was found to be 1150 ± 50 K. The vibrational and rotational temperatures were presumed to be the same, and the relative intensities of all the bands 2–0 through 9–7 for each isotope were predicted

TABLE V

Variation of the Intensity of Overtone Bands with v''

Band	Measured	Calculated
2 - 0	1.0[a]	1
3 - 1	2.7	3
4 - 2	5.7	6
5 - 3	9.1	10
6 - 4	13.7	15
7 - 5	18.6	21
8 - 6	30.1	28
9 - 7	34.1	36

[a] Intensities relative to 2 - 0 = 1.0

assuming equal strength for each band. The relative intensity of lines from different bands was then measured and the intensity "enhancement" from the predicted value was calculated. These were then fitted using a least-squares procedure to yield the intensity enhancements given in Table V.

There have been several papers recently involving the calculation of vibration-rotation intensities (*38–41*), but these generally involve fairly complex expressions including the dipole moment function for the molecule. The data determined here are not sufficiently precise to warrant this type of treatment. The relative intensities are accurate to about 10%. The simple form of the vibrational intensity expression involving Hermite polynomials yields intensities proportional to $(v'' + 1)(v'' + 2)$. The intensities calculated from this formula relative to the 2–0 band intensity (set equal to 1) are given in Table V. It can be seen that the agreement with experiment is good, of the order of the 10% estimated precision.

ACKNOWLEDGMENT

The diode-laser system was purchased with a grant from the Department of Defense University Instrumentation Program.

RECEIVED: November 21, 1988

REFERENCES

1. A. HONIG, M. MANDEL, M. L. STITCH, AND C. H. TOWNES, *Phys. Rev.* **96**, 629–642 (1954).
2. J. R. RUSK AND W. GORDY, *Phys. Rev.* **127**, 817–830 (1962).
3. A. J. HEBERT, F. W. BREIVOGEL, JR., AND K. STREET, JR., *J. Chem. Phys.* **41**, 2368–2376 (1964).
4. S. E. VEAZEY AND W. GORDY, *Phys. Rev. A* **138**, 1303–1311 (1965).
5. A. G. MAKI AND F. J. LOVAS, *J. Mol. Spectrosc.* **95**, 80–91 (1982).
6. A. G. MAKI, *J. Mol. Spectrosc.* **102**, 361–367 (1983).
7. G. THOMSON, A. G. MAKI, AND A. WEBER, *J. Mol. Spectrosc.* **118**, 540–543 (1986).
8. G. A. THOMSON, A. G. MAKI, WM. B. OLSON, AND A. WEBER, *J. Mol. Spectrosc.* **124**, 130–138 (1987).
9. H. JONES AND J. LINDENMAYER, *Chem. Phys. Lett.* **135**, 189–192 (1987).
10. K. HORIAI, T. FUJIMOTO, K. NAKAGAWA, AND H. UEHARA, *Chem. Phys. Lett.* **147**, 133–136 (1988) and *J. Mol. Spectrosc.*, submitted for publication.
11. M. C. DOUAY, A. M. R. P. BOPEGEDERA, C. R. BRAZIER, AND P. F. BERNATH, *Chem. Phys. Lett.* **148**, 1–5 (1988).
12. R. C. HILBORN, T. F. GALLAGHER, JR., AND N. F. RAMSEY, *J. Chem. Phys.* **56**, 855–861 (1972); J. L. CECCHI AND N. F. RAMSEY, *J. Chem. Phys.* **60**, 53–65 (1974).
13. W. KLEMPERER AND S. A. RICE, *J. Chem. Phys.* **26**, 618–624 (1957).
14. W. KLEMPERER, W. G. NORRIS, A. BÜCHLER, AND A. G. EMSLIE, *J. Chem. Phys.* **33**, 1534–1540 (1960).
15. R. S. BERRY, "Alkali Halide Vapors" (P. Davidovits and D. L. McFadden, Eds.), Chap. 3, Academic Press, New York, 1979.
16. A. S. RAGONE, D. H. LEVY, AND R. S. BERRY, *J. Chem. Phys.* **77**, 3784–3789 (1982).
17. S. H. SCHAEFER, D. BENDER, AND E. TIEMANN, *Chem. Phys. Lett.* **92**, 273–278 (1982).
18. P. DAVIDOVITS AND D. C. BRODHEAD, *J. Chem. Phys.* **46**, 2968–2973 (1967).
19. R. S. BERRY AND W. KLEMPERER, *J. Chem. Phys.* **26**, 724–726 (1957).
20. A. W. POTTS AND E. P. F. LEE, *J. Chem. Soc. Faraday Trans. 2* **75**, 941–951 (1979).
21. J. BERKOWITZ, C. H. BATSON, AND G. L. GOODMAN, *J. Chem. Phys.* **71**, 2624–2636 (1979).
22. L. BREWER AND E. BRACKETT, *Chem. Rev.* **61**, 425–432 (1961).
23. E. M. BULEWICZ, L. F. PHILLIPS, AND T. M. SUGDEN, *Trans. Faraday Soc.* **57**, 921–931 (1961).
24. R. L. MATCHA, *J. Chem. Phys.* **53**, 485–495 (1970).

25. A. HINCHLIFFE, *Chem. Phys. Lett.* **70,** 610–612 (1980).
26. P. BRUMER AND M. KARPLUS, *J. Chem. Phys.* **58,** 3903–3918 (1973).
27. J. SHANKER AND H. B. AGRAWAL, *Canad. J. Phys.* **58,** 950–956 (1980).
28. J. SHANKER, H. B. AGRAWAL, AND G. G. AGRAWAL, *J. Chem. Phys.* **73,** 4056–4060 (1980).
29. J. SHANKER AND H. B. AGRAWAL, *Canad. J. Phys.* **60,** 1187–1192 (1982).
30. B. T. GOWDA AND S. W. BENSON, *J. Phys. Chem.* **86,** 847–857 (1982).
31. J. E. SZYMANSKI AND J. A. D. MATHEW, *Canad. J. Phys.* **62,** 583–589 (1984).
32. M. KUMAR, A. J. KAUR, AND J. SHANKER, *J. Chem. Phys.* **84,** 5735–5740 (1986).
33. E. S. RITTNER, *J. Chem. Phys.* **19,** 1030–1035 (1951).
34. G. VAN HOOYDONK, *J. Mol. Struct.* **105,** 69–90 (1983).
35. G. GUELACHVILLI AND K. NARAHARI RAO, "Handbook of Infrared Standards," Academic Press, San Diego/Orlando, 1986.
36. J. L. DUNHAM, *Phys. Rev.* **41,** 721–731 (1932).
37. J. K. G. WATSON, *J. Mol. Spectrosc.* **80,** 411–421 (1980).
38. C. CHACKERIAN, JR., AND R. H. TIPPING, *J. Mol. Spectrosc.* **93,** 237–244 (1982).
39. R. H. TIPPING AND J. F. OGILVIE, *J. Mol. Spectrosc.* **96,** 442–450 (1982).
40. J.-P. BOUANICH, NGUYEN-VAN-THANH, AND I. ROSSI, *J. Quant. Spectrosc. Radiat. Transfer* **30,** 9–15 (1983).
41. J.-P. BOUANICH, *J. Quant. Spectrosc. Radiat. Transfer* **37,** 17–46 (1987).